Automation in Construction 96 (2018) 366–377

Contents lists available at ScienceDirect

Automation in Construction

journal homepage: www.elsevier.com/locate/autcon

Automated specification of steel reinforcement to support the optimisation of RC floors

S. Eleftheriadis[a,b,*], P. Duffour[c], B. Stephenson[d], D. Mumovic[a]

[a] UCL Institute for Environmental Design and Engineering, University College London, UK
[b] Department of Computer Science, University College London, UK
[c] Department of Civil, Environmental & Geomatic Engineering, University College London, UK
[d] Price & Myers LLP, 37 Alfred Place, WC1E 7DP London, UK

ARTICLE INFO

Keywords:
Design
Automation
Optimisation
RC structures
Steel reinforcement
Floors

ABSTRACT

A Building Information Modelling (BIM)-enabled computational approach was presented in this paper for the automated specification of steel reinforcement to support the optimisation of reinforced concrete (RC) flat slabs. After importing slab geometries from BIM, the proposed procedure utilised internal forces output from Finite Element Model (FEM) to map required reinforcement in two stages. In the first stage, the reinforcement specifications matched the spatial resolution of the FEM. In the second, the reinforcement was adjusted by imposing constructability functions to limit the number of arrangements in terms of zones and bar spacing. The aim of the paper was to investigate the parametric capabilities of the proposed approach in the context of an optimisation model for the generation of material-efficient structural designs. Numerical examples were presented to demonstrate the efficiency of the automated specification procedure. The material efficiency and the design complexity of the developed reinforcement configurations were also assessed against a conventional solution under realistic design conditions.

1. Introduction

Cast in situ reinforced concrete (RC) structures are prevalent in small and medium residential and office buildings. However, their detailed design and construction remain relatively low-tech and labour intensive. The design of these structures involves specifying the placement and size of reinforcing bars within the concrete matrix. This phase of the design usually follows an iterative process, in which structural engineers use a manual trial-and-error approach to find a sufficiently safe and economical structural solution [1,2].

However, the trial-and-error method often demands considerable amount of time and effort [3,4]. Most structural engineering problems could be formulated as optimisation problems that achieve optimum structural performance whilst satisfying conflicting design constraints [5]. Reinforcement design is no exception and designing it this way would achieve both automation and optimisation at the same time [4]. This paper proposes a numerical process to achieve this.

Structural optimisation techniques [6] have been applied in many fields of engineering [7–12] however their uptake in engineering practices is sometime met with some resistance. Common reasons for this reluctance include issues such as training and attitude, modelling development and post-processing procedures, data sharing in multidisciplinary frameworks and algorithm selection among others according to a recent study that surveyed to what extend engineering companies in the UK use computational optimisation approaches [13].

Despite practicing engineers' expertise and experience, conventional structural design processes often result in sub-optimal solutions [14]. New design processes that increase the adoption of practical optimisation techniques by structural engineering practitioners are still necessary [15]. Developments within Building Information Modelling (BIM) technologies and computational systems are expected to enhance the integration of optimised structural designs with more efficient design [16] and construction [17–19] procedures. More specifically, Chi et al. [20] recognised five areas that will become more relevant with the development of BIM technologies in the context of structural engineering:

- Adoption of structural optimisation during the early design stages
- Parametric design specifications for enhanced sustainability performance
- Intuitive decision-making models supported by advanced visualisation techniques

* Corresponding author at: 14 Upper Woburn Place, London WC1H 0NN.
E-mail address: ucabele@ucl.ac.uk (S. Eleftheriadis).

https://doi.org/10.1016/j.autcon.2018.10.005
Received 27 June 2018; Received in revised form 1 October 2018; Accepted 3 October 2018

- Numerical applications in realistic engineering examples
- Amplified collaboration and communication between design teams

The current study investigates how Chi et al.'s [20] insights could be implemented in the context of RC building structures with flat slabs, which are a very commonly used floor system with reinforced concrete structures.

In the optimisation of flat slabs [21], the focus is on the careful selection of slab thicknesses as the concrete in the slab constitutes the largest proportion of the floor material [22]. However, slab thickness optimisation is often limited by constructability constraints, which dictate a small finite set of slab thickness options. On the other hand, the optimisation of reinforcement could be achieved in various ways by engineering practitioners, and could lead to significant material savings. In a recent flat slab optimisation study, the reinforcement accounts for approximately 25% of the total material and construction costs in the floor [21]. Similar figures have also been reported in other studies conducted by Sahab et al. [23] and Eleftheriadis et al. [22,24] with flat slab systems.

Previous studies have focused on the reinforcement optimisation of different structural frames mainly without the implementation of BIM technologies [25–27]. However, in a recent study by Mangal & Cheng [4] the reinforcement (longitudinal and shear) of RC frames (beams and columns) was optimised using a BIM-based approach. Little attention was given on the automation of reinforcement specifications to support the optimisation of RC flat slabs.

In this study an automated reinforcement specification process is proposed to effectively support the optimisation of RC flat slabs, which is a structural system that is used extensively in the UK and many other countries. Section 2 describes the computational processes used in this study to automate the specification of steel reinforcement. Numerical applications and the validation of the proposed computational model are presented in Section 3. The paper concludes with discussion in Section 4 and conclusions in Section 5.

2. Methods and models

2.1. Optimisation framework and context

The BIM-based approach that was initially proposed by Eleftheriadis et al. [22] for the optimisation of RC flat slabs and columns using single objective functions for cost and embodied carbon, was extended to simultaneously evaluate multiple objectives deploying a bespoke NSGA-II algorithm with a FEM engine [24]. In this paper, special attention is given to the computational modules and processes of the optimisation approach described in [24] that are responsible for the automated reinforcement specification of RC floor structures. The specification of the reinforcement is an important component of the optimisation analysis enabling the computation of structural material quantities necessary for the cost and embodied carbon calculations. Typically, the specification of reinforcement in RC floors is completed by structural engineers during the early design stages using aggregate reinforcement rates (the quantities are given kg/m^3). The main aim of the proposed reinforcement specification procedure was to ensure that detailed yet practical reinforcement topologies (layouts) and schedules (quantities) are utilised not only for optimisation purposes but also for the refinement of construction drawings and design information at detailed design stages by the structural engineers through dedicated BIM interoperability [24]. Because the optimisation of a structure involves multiple iterations until a set of optimised solutions is adequately obtained (in some cases thousands of iterations might be required depending on the complexity of the building case [24]), the detailed analysis of the slab reinforcement should be automated in an efficient and robust way. The general workflow of the optimisation is shown in Fig. 1.

The optimisation procedure begins by querying building and geometric information directly from a BIM model into the FEM engine. To support the reinforcement analysis for the slab component a set of customised algorithms was constructed in juxtaposition with the FE engine. If the relevant code constraints and limit states are satisfied after the FE analysis, material schedules for the concrete and the steel reinforcement as well as the reinforcement zones in the slab are specified. The same reinforcement specification procedure is repeated multiple times for the design optimisation of the slab using the NSGA-II until a set of optimised solutions is obtained and visualised in the Pareto front. Thorough review of the optimisation principles as well as results from numerical examples can be found in [24].

2.2. Automated reinforcement analysis

The proposed automated design specification process comprises three main stages:

1) Processing data from BIM so that the floor system can be analysed with a finite element (FE) model;
2) Generating refined reinforcement maps that match the mesh size of the finite element model;
3) Simplification and smoothing of the refined mesh to ensure it is practical to build.

In this paper, Autodesk Robot Structural Analysis (RSA) 2016 was used for the FE calculations and Autodesk Revit for BIM as these are currently very commonly used in the industry [16]. The entire computational process is driven automatically through code developed in C# using the Application Programme Interface (API) of RSA and Revit. The project requirements define the material properties, load cases and support coordinates which are directly transferred from BIM to the FE model via the API. The slab-column connections are modelled in the FE model assuming pinned supports. The limit state checks are specified based on national or international codes. In this study, all structural limit states were checked according to Eurocode 2 (EC2) [28,29].

Once the structural model is established in RSA, the calculations leading to the estimation of the slab reinforcement begin. Firstly, detailed required reinforcement maps are calculated at the resolution of the finite element mesh size. These refined maps are then smoothed out and simplified into practical reinforcement bar specifications. At the end of this process, the reinforcement schedule as well as the detailed reinforcement weight of the slab are obtained. Fig. 2 shows the general computational workflow including the necessary processes for the calculation of the required and the specified reinforcement.

2.3. Required reinforcement calculations

Using the FEM output, the required reinforcement is calculated as an area of steel per unit length for top and bottom reinforcement in both directions at each node of the finite element mesh. An example of a map showing this required reinforcement is presented in Fig. 3 for a generic slab component.

The map in Fig. 3 highlights the areas where no reinforcement is required as well as the areas where reinforcement is needed based on the code restrictions. As the reinforcement follows the FE mesh, this map represents the smallest amount of steel that must be provided for a given FE mesh size. Punching shear reinforcement has not been specified at this stage of the project and thus, it is not included in the scope of this study.

Coons' method [30] is used to generate the finite mesh in the slab, and the Wood & Armer method [31] is used in the calculation of the moment for the required reinforcement in the slab. The finite element mesh size can be adjusted by the user based on the project requirements. Herein it was initialised using the value the structural engineers used (0.5 m) in the tested building scenario under examination. This allowed a direct comparison and assessment of the conventional designs with the computer-generated scenarios presented in Section 3. Details

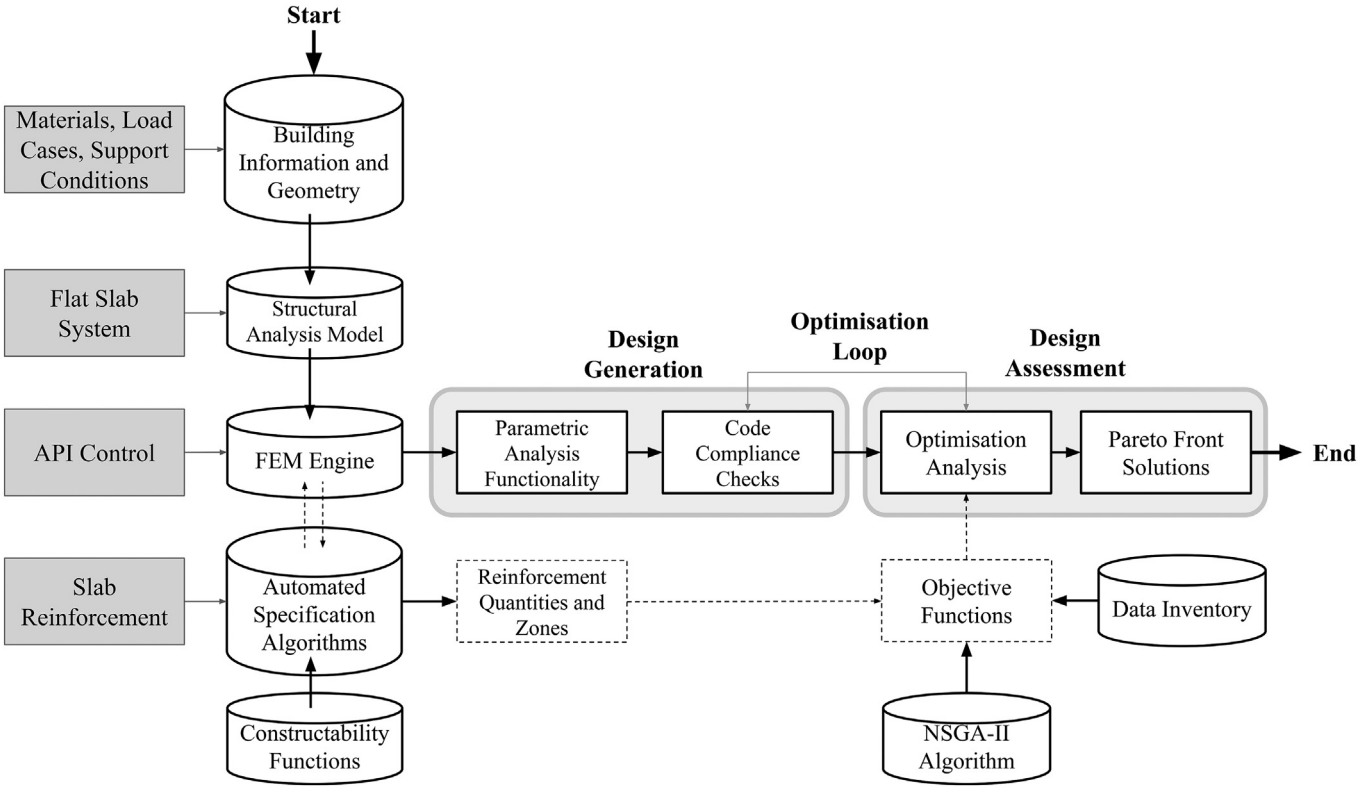

Fig. 1. Suggested workflow for the optimisation of RC floors using the approach described in [24]. The automated specification algorithms are part of the FEM engine and utilised for the computation of reinforcement quantities, which are subsequently used in the objective functions of the NSGA-II algorithm.

on the mesh sensitivity and the computational performance of the algorithm can be found in [24].

These required reinforcement maps are used to compute the minimum and maximum values of required reinforcement for each element (hereafter called cell) in the FE model. For either top or bottom and for a given direction, the minimum value from all the FE cells is used to estimate the basic reinforcement mesh across the slab whilst the difference between the maximum and the minimum values is used to calculate the additional reinforcement in the zones where it is necessary (typically above the columns or mid-span areas).

An additional function was incorporated in the proposed computational process to reduce the peak bending moments obtained from the FEM that typically appear over column supports. This function decreases the risk of reinforcement overestimation in the slab using the column strip approach based on Annex I EC2 [29]. A section is taken across the bending moment diagram (i.e. in the y direction for moments in the x direction) at the face of the column.

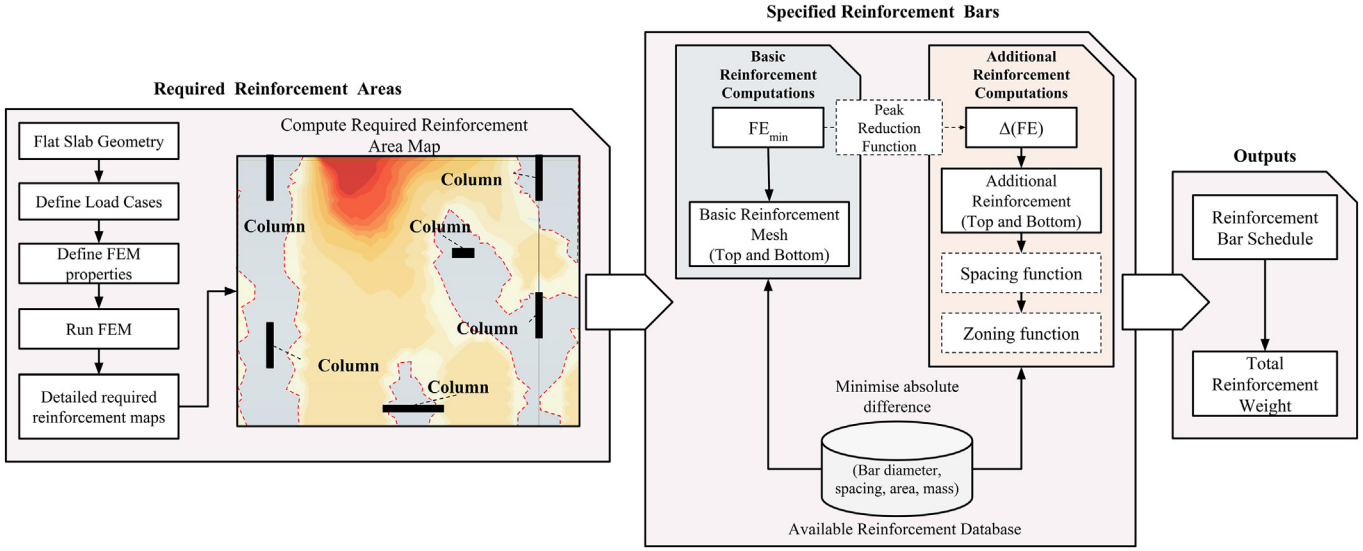

Fig. 2. Automated reinforcement computations flowchart. The computations are organised in three main components: 1) Computation of required reinforcement areas using geometric, building and loading data, 2) Computation of basic reinforcement mesh and additional reinforcement bars using various algorithmic functions, 3) Computation of reinforcement schedules and material lists.

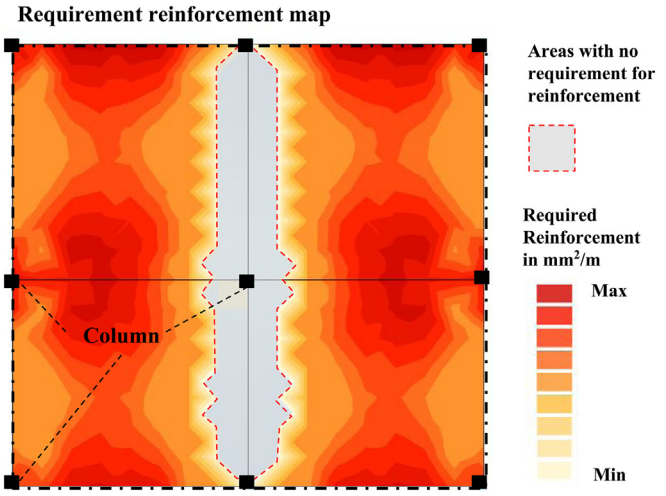

Fig. 3. Fine reinforcement map in a slab component showing the gradient of required reinforcement as computed by FEM. This is a common way to visualise the areas in a slab that require more reinforcement (dark red zones). For any given slab, four maps like that are typically computed (2 maps in each direction of reinforcement, for top and bottom meshes). (For interpretation of the references to colour in this figure legend, the reader is referred to the web version of this article.)

2.4. Steel reinforcement specification

Once the required reinforcement maps are calculated the reinforcement bar specification is computed using a database of reinforcement options. The database is encoded using a text file which includes information about the diameters of the bars, the spacing between bars, the reinforcement areas and the steel weight. The ultimate output from this process will be the specified reinforcement which will almost always be higher than the required reinforcement produced by the first stage.

The assignment process for the specified reinforcement is executed using the RSA API and the FEM results from the required reinforcement calculations. A custom algorithm queries the text file and identifies the option that matches more closely to the minimum required reinforcement values. The aim of this recursive procedure is to minimise the absolute difference between the required reinforcement area values at every finite element node and the reinforcement area value of the data points in the text file with the reinforcement options.

This process is repeated for all the finite element nodes in the slab. The same specification process is carried out for the assignment of the reinforcement in the basic steel mesh as well as the additional reinforcement mesh. The detailed functionalities associated with the computation of the basic and the additional reinforcement (spacing and zoning) are presented in the subsequent sections.

An example of the assignment algorithm is shown in Fig. 4. In a floor plate with required reinforcement of 322 mm^2/m, the algorithm finds that ø10 at 225 mm (349 mm^2/m) would be the most suitable reinforcement option as it minimises the difference between the required reinforcement and the available options in the database. To ensure that the specified reinforcement is safe the computed difference needs to be a positive number (> 0).

Once an appropriate reinforcement option is found the algorithm stores the corresponding bar spacing as it is used in the spacing function of the additional reinforcement (See Section 2.5). Finally, the total weight of the basic mesh is calculated multiplying the mass factors integrated within the database given in kg/m^2 and the entire slab area in m^2. A similar reinforcement assignment process is implemented for the estimation of the additional reinforcement.

Fig. 5 shows the one-to-one weight mapping of additional reinforcement for a simplified slab component in all reinforcement directions top and bottom. The number shown on each cell corresponds to the weight factors obtained from the reinforcement database and presented in the previous section. For example, the value 3.6 kg/m^2 corresponds to ø12 at 250 mm or the value of weight factor 2.5 kg/m^2 corresponds to ø10 at 250 mm. The algorithm assigns a value of 0 where no additional reinforcement is needed. The total weight of the reinforcement in the slab is computed by multiplying the obtained weight factors with the cell areas and finally by adding all the cell weights together. The same maps are also generated for the basic reinforcement mesh but with only one reinforcement type applied in all the cells.

2.5. Constructability constraints

Two constructability constraint functions are implemented to enhance the practical applicability of the computational solutions: 1) spacing function, and 2) zoning function.

2.5.1. Spacing function

The spacing function ensures that the additional reinforcement bars are placed between the bars of the basic mesh by preserving equal distances. This functionality significantly reduces the fitting and installation time of reinforcement bars on site. In the spacing function, the bar spacing specified for the computations of the basic mesh is maintained and re-used in the additional reinforcement calculations. The algorithm checks the reinforcement database for the combination options with the defined spacing and then identifies the smallest safe reinforcement option.

Fig. 6 shows the implementation of the spacing requirement in a notional slab panel. Maintaining the same spacing ($d_{add} = d_{basic}$) allows the additional bars (in red lines) to be placed at the same interval as the basic mesh bars which are shown with black lines, ensuring consistent spacing throughout the slab.

2.5.2. Zoning function

The zoning function simplifies the one-to-one mapping for the additional reinforcement by altering the selection of bars on adjacent FE cells to reduce short length bars that often complicate reinforcement fixing on site.

Fig. 7 illustrates how the zoning algorithm is implemented on an example slab component based on the horizontal direction of reinforcement. A representative scenario is shown for the highlighted cells in row 10. All the cells in columns 9–16 are analysed to proceed with the cell adjustments. For example, in the entire column 9 no reinforcement is necessary, and as a result, this cell is not altered. For cells 10–16, the maximum value is obtained (6.32 which corresponds to ø16 at 250 mm of reinforcement) and the neighbouring cells are assessed against that value. If the value in the remaining cells are different from the maximum value, then they are updated accordingly. The same process is applied in the X and Y directions, top and bottom reinforcement.

3. Numerical examples

To test the automated specification method the case study from [22] was used. Six optimised reinforcement designs are generated by the computational process following six design scenarios involving various constructability constraints. These were analysed and compared to a conventional design produced by practicing engineers (without automation or any formal optimisation). The computational method utilises the same geometric properties and the same project constraints for the structural system as the conventional design.

3.1. Computational scenarios

Different simulation cases were analysed to evaluate the behaviour

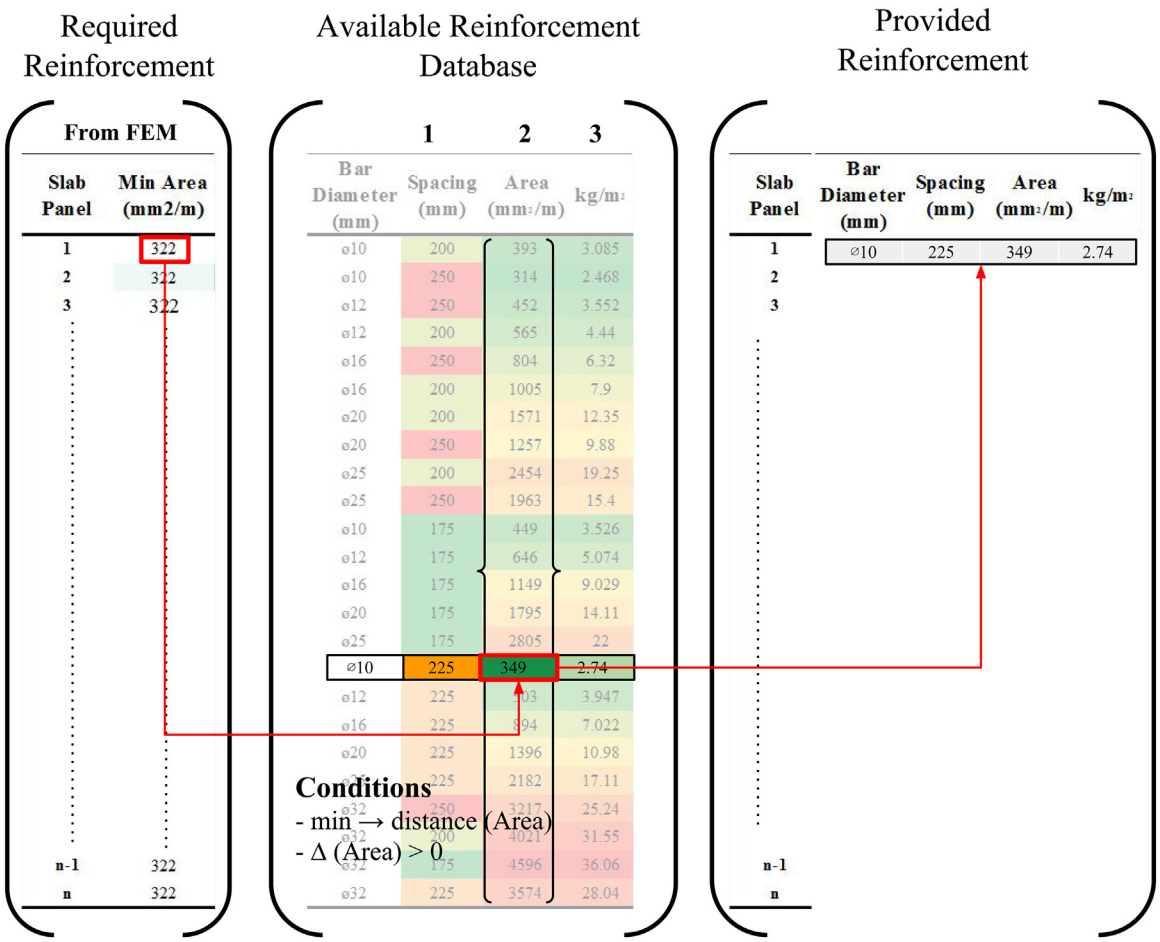

Fig. 4. The assignment process utilises required reinforcement data obtained from FEM and a detailed reinforcement database which includes various reinforcement combinations including data for bar diameters, spacing between bars, reinforcement area and weight factors. The algorithm uses two main operations before computing the provided reinforcement. The algorithm searches for the option in the database that closely matches (min difference) the minimum required reinforcement, whilst ensuring that the difference is a positive number to avoid the selection of a suboptimum option.

of the computational constraints. Table 1 summarises the six different simulation scenarios that were tested in this study to assess how well the computational model performs against conventional practice. All six scenarios are evaluated by computing the total reinforcement weight in the slab. The classification of the scenarios is based on two reinforcement databases (D1, D2) and spacing along with zoning functions.

Database D1 consists of 24 reinforcement options using discrete sets of inputs for the bar sizes and the reinforcement spacing. In this database (D1), the bar sizes vary from ø10mm to ø32mm and the spacing between bars varies from 175 mm to 250 mm with 25 mm increments. The intention behind this classification is to help the algorithm identify reinforcement combinations that are closer to what practicing engineers would use in real projects.

However, these constraints can be superseded and more or different reinforcement combinations could be implemented if desired. This would yield more efficient results as the distance between the actual reinforcement option and the required reinforcement could be further optimised. To investigate how much these common spacing variables affect the calculation results a more detailed databased (D2) of 138 reinforcement options is also developed. D2 includes the same bar diameters as D1, but with more spacing options which varying from 50 mm to 250 mm with 10 mm increments.

Fig. 8 shows the number of reinforcement options for both databases with their corresponding areas of reinforcement. It can be observed that five times more reinforcement options are available in D2 when compared to D1's maximum capacity (4596 mm^2/m).

In scenarios 1 and 2, the spacing and zoning functions are switched off, which means that the computation of the reinforcement would be the most optimum in terms of weight as no constructability constraints are utilised. These scenarios would be better suited for automated construction and fabrication processes such as reinforcement mats, which allow variable spacing and bars to be used. Scenarios 3 and 4 utilise the zoning function, which allows the additional reinforcement bars to be organised based on constructability rules but not the spacing constraint. Finally, scenarios 5 and 6 fully utilise both the spacing and zoning functions. The results are expected to be similar to the results obtained from the conventional design process.

3.2. Conventional design

Fig. 9 shows the general floor layout and the BIM model of the structural system. The structure comprises 275 mm flat slabs with a 250 mm thick central core. The column grid consists of variable 3 m × 3 m bay configurations on both directions. In the X-direction, the grid includes 6.5 m, 5 m and 4.5 m spans, whereas in the Y-direction, the spans are 5 m, 4 m and 6 m. The columns are designed by the project engineers, and they are 400 × 400 mm. The combined dead load of the structure (DL), superimposed load (SDL) on the slab is 2.5 kN/m^2 and imposed load (IL) is 7.5 kN/m^2. Concrete strength of C32/40 and C50 were chosen for the slab and columns respectively, whereas steel grade of B500 was used for the reinforcement bars.

The plans in Fig. 10 show the top and bottom required reinforcement maps in both directions for the slab of the tested building. Fig. 10

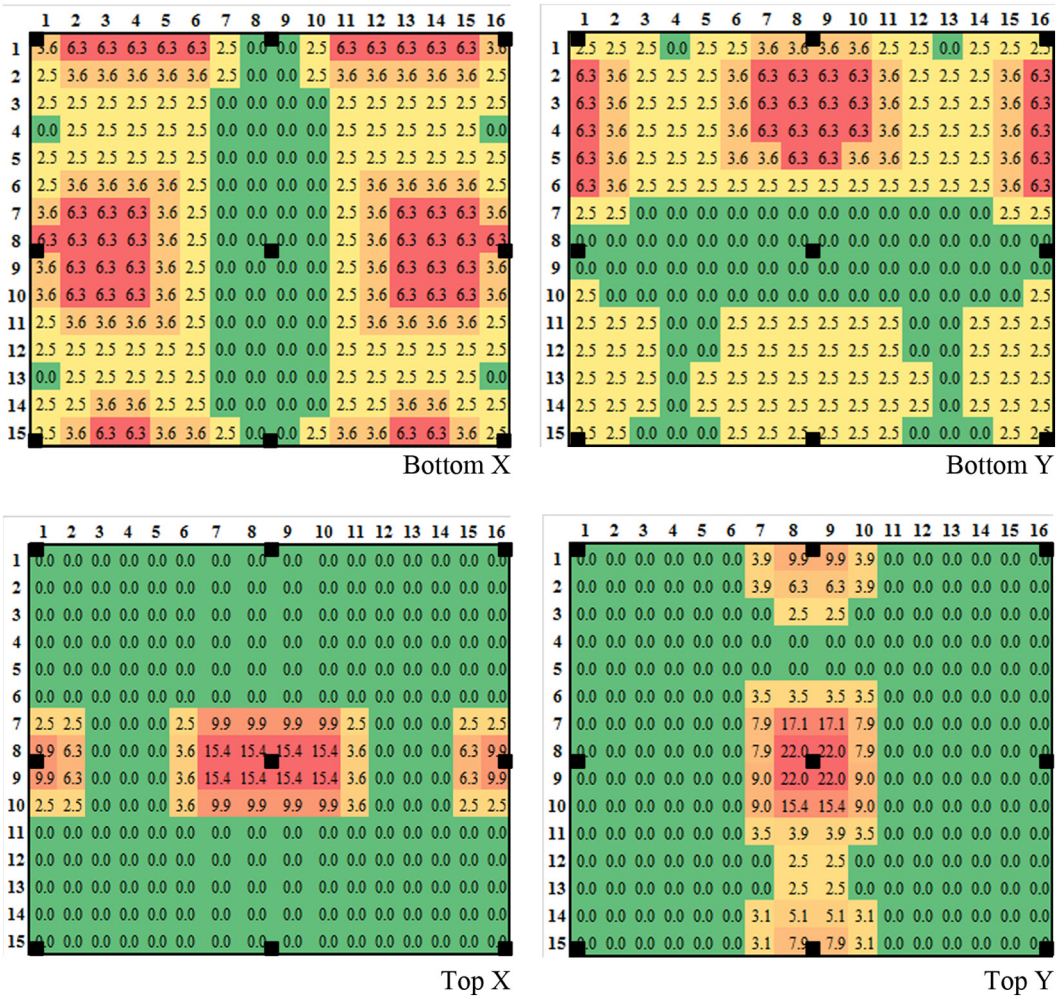

Fig. 5. One-to-one mapping of additional reinforcement with weight factors given in kg/m^2 (cell sizes 0.5mx0.5 m) for all four reinforcement directions. The figure highlights that the proposed approach can achieve a high level of customisation when it comes to the selection of additional reinforcement to closely match the required reinforcement maps described in Fig. 3. For each FE cell additional reinforcement bars are computed following the assignment process defined in Fig. 4.

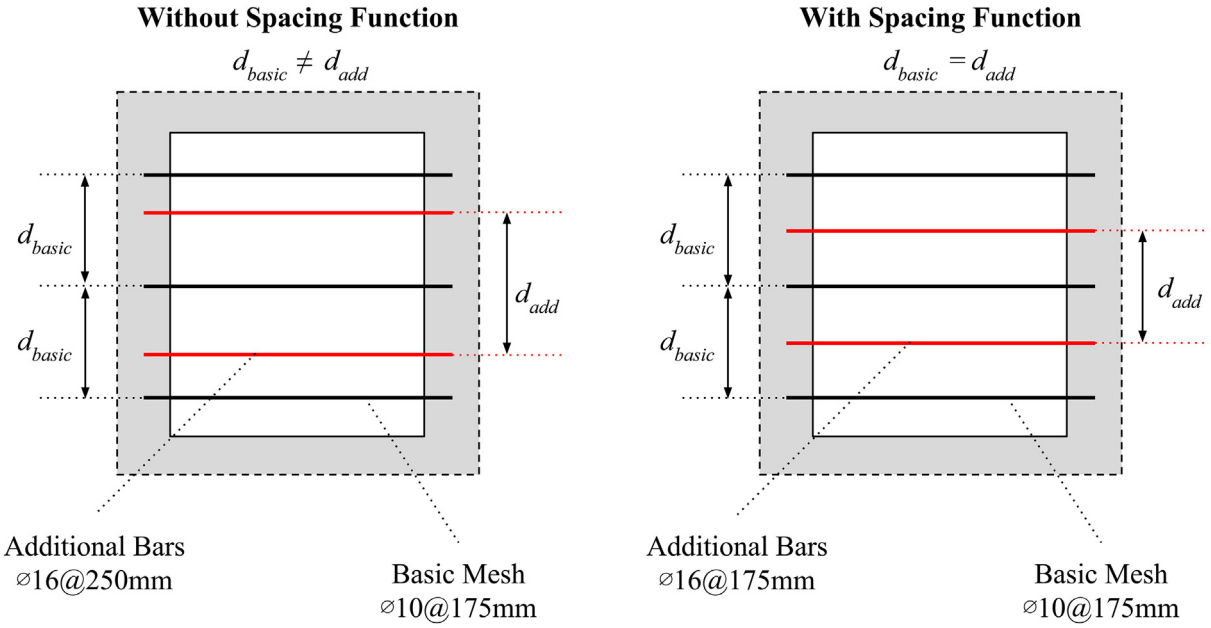

Fig. 6. Spacing function to adjust the additional reinforcement positions in the slab. This function ensures that d_{add} is equal to d_{basic}, which helps improve constructability and reduce errors on site.

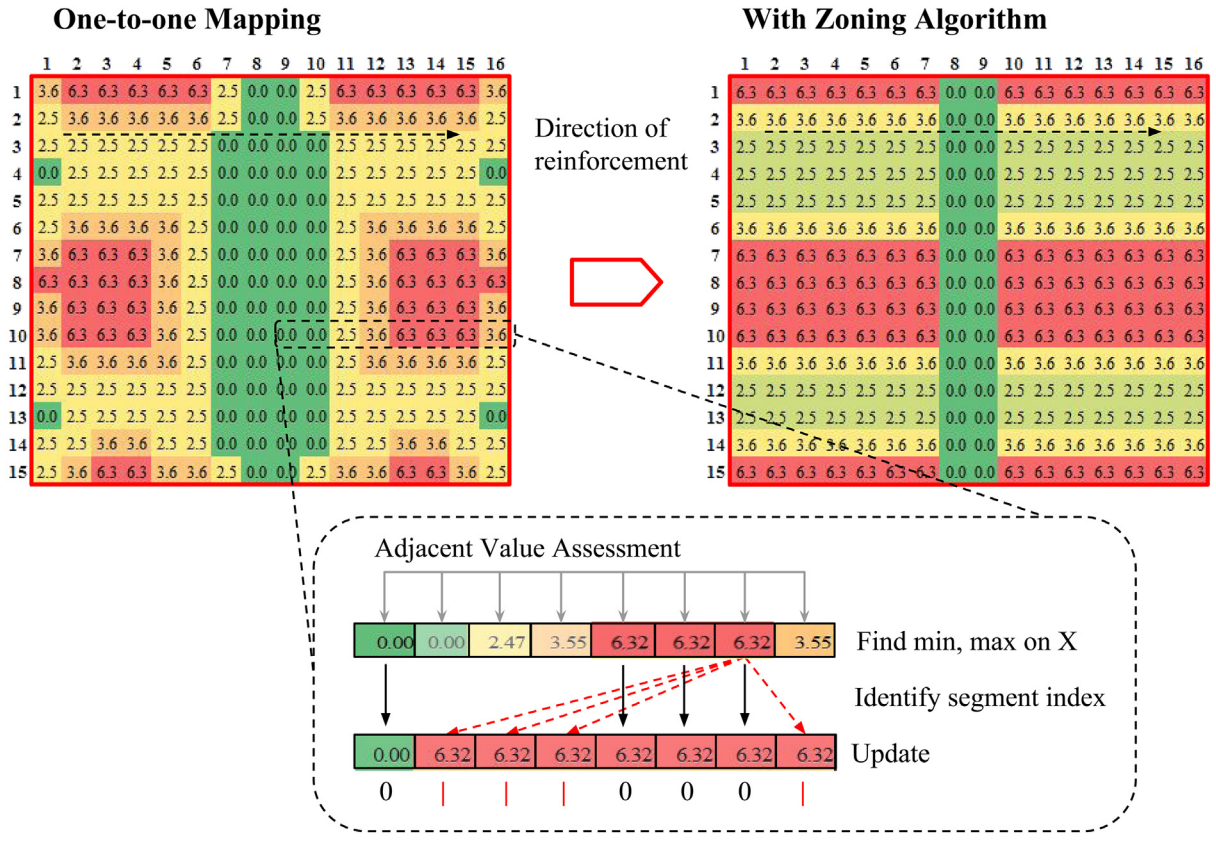

Fig. 7. Zoning algorithm for the computation of additional reinforcement using a logic implemented by engineering practitioners to simplify the reinforcement topologies.

Table 1
Simulation scenarios summary using different reinforcement databases and algorithmic components.

	1	2	3	4	5	6
Reinforcement database	D1	D2	D1	D2	D1	D2
Spacing constraint					✓	✓
Peak reduction	✓	✓	✓	✓	✓	✓
Zoning constraint			✓	✓	✓	✓

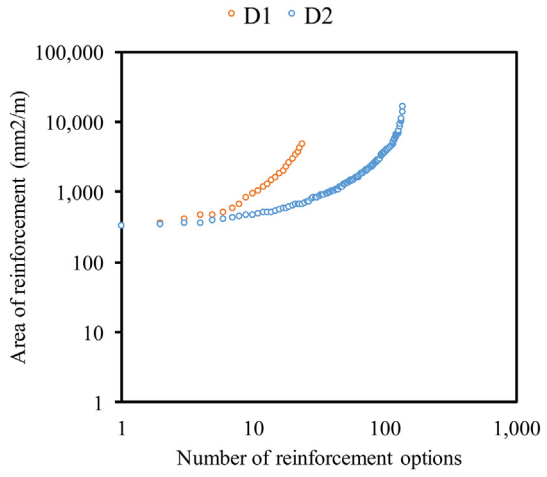

Fig. 8. Reinforcement data points for D1 and D2 databases (Logarithmic scale). The horizontal axis shows the number of different reinforcement options in the two databases D1 and D2. The vertical axis shows the corresponding area of reinforcement for every reinforcement option.

a and b are the maps for the bottom reinforcement. Fig. 10 c and d on the other hand, show the top reinforcement. The areas highlighted in red represent the zones with higher reinforcement requirements compared to the areas highlighted in orange or yellow. The required reinforcement maps from the FEM are used to estimate the actual reinforcement in the slab. The large peaks observed above the columns shown in Fig. 10 c and d are distributed across a larger area of column strips by averaging the bending moments as explained in Section 2.3.

The reinforcement specified by the project engineers is summarised in Table 2. The basic mesh for the top and the bottom reinforcement is ø10 at 200 mm, whereas the additional top reinforcement is ø16 at 200 mm and the additional bottom reinforcement is ø10 at 200 mm. The total weight of the reinforcement in the slab is 4502 kg excluding any laps. The conventional design includes spacing of 200 mm, which is commonly used in practice, and it contains only 2 different bar diameters (Ø10, Ø16). The number of different bars is used in this study as a measure of design complexity when assessing the optimised design options.

Fig. 11 highlights the zoning strategy of the reinforcement in the conventional design. A basic mesh is applied both to top and bottom reinforcement, and additional bars are added where more reinforcement is required.

3.3. Verifications checks

3.3.1. Weight assessment

A simple check was carried out to ensure the feasibility of the computational process outputs. This was carried out by comparing the reinforcement weight and layout for the conventional design to that produced by the automated process imposing constraints on bar diameters and spacing. A simplified reinforcement database with 6 available bar diameters (ø10, ø12, ø16, ø20, ø25, ø32) and fixed spacing

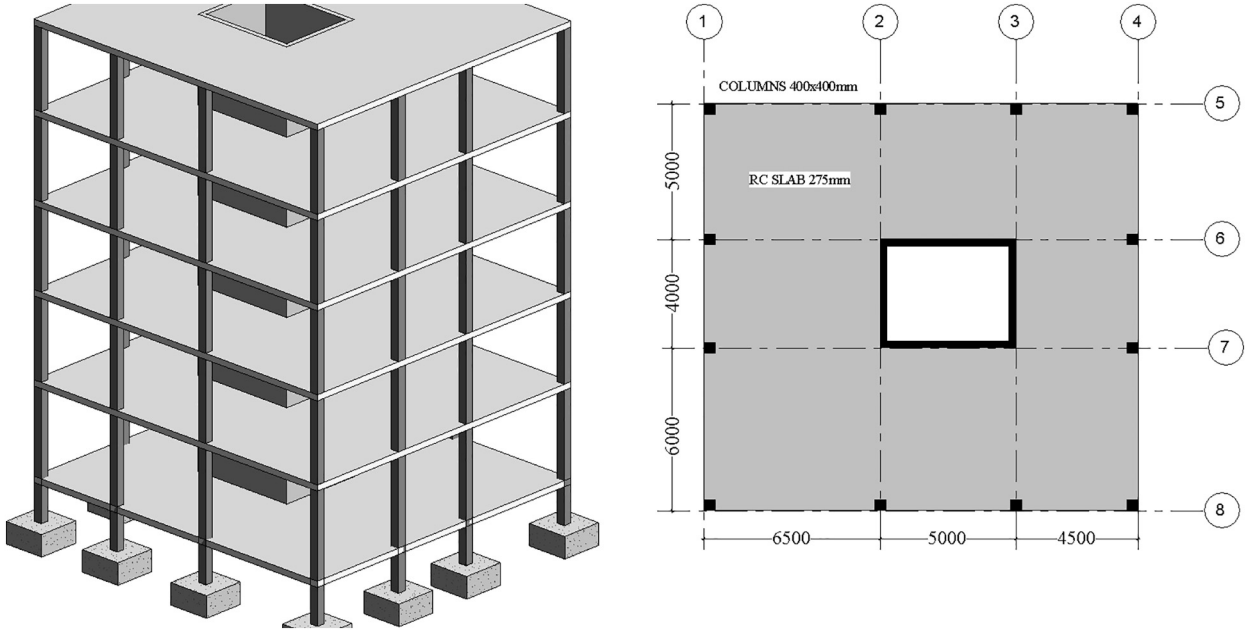

Fig. 9. Structural BIM model and slab layout for the tested building scenario.

between bars (200 mm) was imposed as these are the alternatives the project engineers used in their actual design proposal. The reinforcement in the slab was calculated using the computational process. The total weight of reinforcement from the computational method for this simplified database is 4517 kg which is a very close match (≈100%) to that of the conventional design. The reinforcement layouts produced by the computational design were also assessed against the conventional design. Fig. 12 shows an example of that comparison for the bottom reinforcement in the X direction.

The reinforcement layout of the computational design (left) matches exactly the one the engineers specified in the conventional design (right). In both designs the basic mesh consists of ø10 bas at 200 mm spacing but with a few differences in the additional bar diameters as highlighted in Fig. 12. The conventional design uses only ø10 bars (lines in blue) for the additional reinforcement but in the computational design 83% of the additional bars is ø10 with the remaining bars being ø12 (lines in green) and ø16 (lines in purple).

This difference is mainly attributed to the accurate representation of the bending moments shown in Fig. 10 a. This is also a good example that demonstrates how the engineering practitioners often rationalise the specification of reinforcement across the entire slab. Similar behaviour of the computational process was observed for the reinforcement specification on the rest of the reinforcement layouts (top and bottom). Overall, it can be observed that the computational design can effectively create a very close approximation of realistic reinforcement schedules and layouts.

3.3.2. Peak reduction

Fig. 13 a shows the reinforcement options for top and bottom meshes in both directions for the building without reducing the bending moment peaks. If the peaks are not effectively treated, the bars on top reinforcement can reach up to 25 mm in diameter which is obviously a conservative value and is typically to be avoided in this kind of structures unless completely necessary. To eliminate these situations, the peak reduction subroutine described in Section 2.3 was implemented to reduce the peak moments on the column by evenly distributing them on the column strip zones. The resulting conditions for the top reinforcement bars and the adjusted peak reinforcement requirements are shown in Fig. 13 b. Using this algorithmic approach, the largest bar diameters which were observed above the columns zones can be effectively reduced from 25 mm to 20 mm, which is a more realistic solution for the given building and load case.

3.4. Simulation results

3.4.1. Material use

Fig. 14 summarises the total weight of the reinforcement in the slab for the six scenarios as obtained from the computational process against the conventional design. Results show that the selection of reinforcement database has a small impact on the weight for the same constructability constraints. The database with more detailed reinforcement options (D2) can yield more optimised designs by only 2% when compared to database D1 with more limited reinforcement options.

Fig. 15 shows an example of this application considering the required reinforcement data from all the FE cells in the slab for the bottom reinforcement (X direction). Despite the more accurate mapping of the required reinforcement with database D2, its total reinforcement weight is marginally improved against D1 due to the small differences obtained between the two provided reinforcement options and the small occurrence of those differences. The most material-efficient options emerged in the scenarios where the constructability functions were disabled (in scenarios 1 and 2).

The results show significant material savings, which can be attributed to the algorithm's one-to-one mapping of the required reinforcement. The scenario using the D1 database reduces the total weight of reinforcement in the slab by 21% when compared to the conventional design and by 23% when using the D2 database. Furthermore, in scenarios 3 and 4 the total reinforcement weight is higher than scenarios 1 and 2 by approximately 12% due to the rationalisation of reinforcement occurred by the zoning function. On the other hand, scenarios 5 and 6 closely match the weight estimations for the conventional design by 3% and 5% respectively. This suggests that the zoning and spacing algorithms are effective at generating practical reinforcement designs that are close to those obtained through conventional practice.

3.4.2. Design complexity

The design complexity of the tested scenarios is assessed using a measure of the total number of the different reinforcement types implemented in each design. Currently engineering practitioners try to minimise the number of different bar diameters and spacing types used

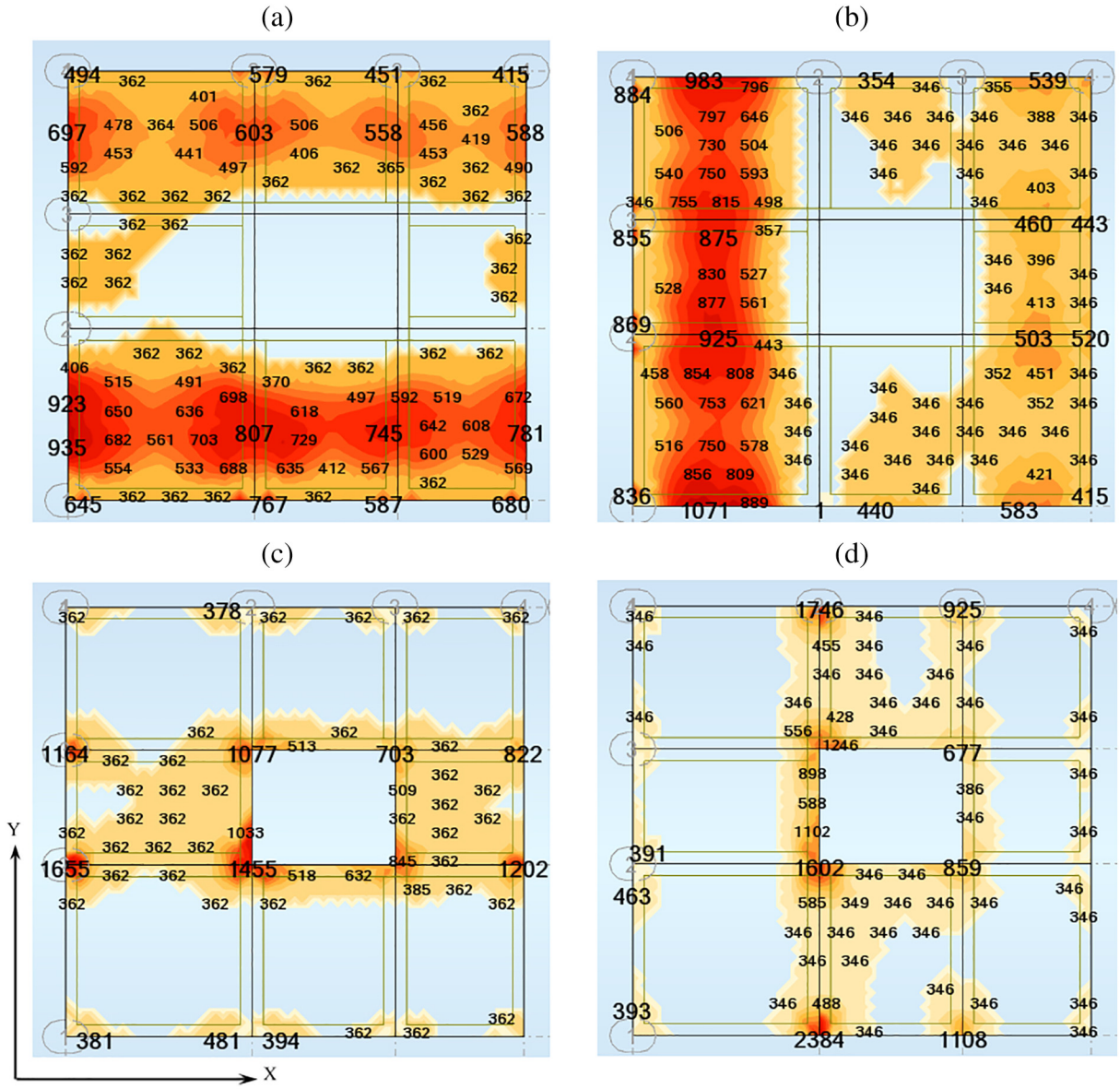

Fig. 10. Maps showing the required areas of reinforcement for (a, b) bottom, (c, d) top reinforcement as obtained from the FEM model – Results displayed in mm^2/m.

to ease fabrication on site. It is expected that a larger number of reinforcement types would result in more optimised designs due to a more accurate representation of the required reinforcement maps. Fig. 16 shows the total reinforcement weight for the six scenarios in ascending weight order against their corresponding number of reinforcement types.

Restricting the database of available reinforcement to commonly used diameters and arrangements is crucial. Scenario 2, which is the most optimum configuration in terms of reinforcement weight uses 35 different reinforcement types. Instead, scenario 1 achieves slightly worse performance by approximately 2% using significantly fewer reinforcement types (13 in total).

A similar behavior in the model is observed in scenarios 3 and 4 which implies the importance of the spacing function for the reduction of the design complexity of the reinforcement design. On the other hand, in scenarios 5 and 6, the constraints imposed by the zoning and spacing functions seem not to affect the total number of reinforcement types used in the slab. Thus, the selection of the reinforcement database becomes less relevant. Overall, it can be observed that more complex designs result in more material-efficient solutions. Therefore, understanding the design requirements and building conditions is necessary when setting up the model.

Table 2
Conventional reinforcement quantities.

	Basic mesh	Weight factors (kg/m^2)	Weight (kg)	Additional bars	Weight factors (kg/m^2)	Weight (kg)
Bottom reinforcement	Ø10 at 200 mm	3.085	1357	Ø10 at 200 mm	3.085	777
Top reinforcement	Ø10 at 200 mm	3.085	1357	Ø16 at 200 mm	7.9	1011
			2714			1788
Total						4502

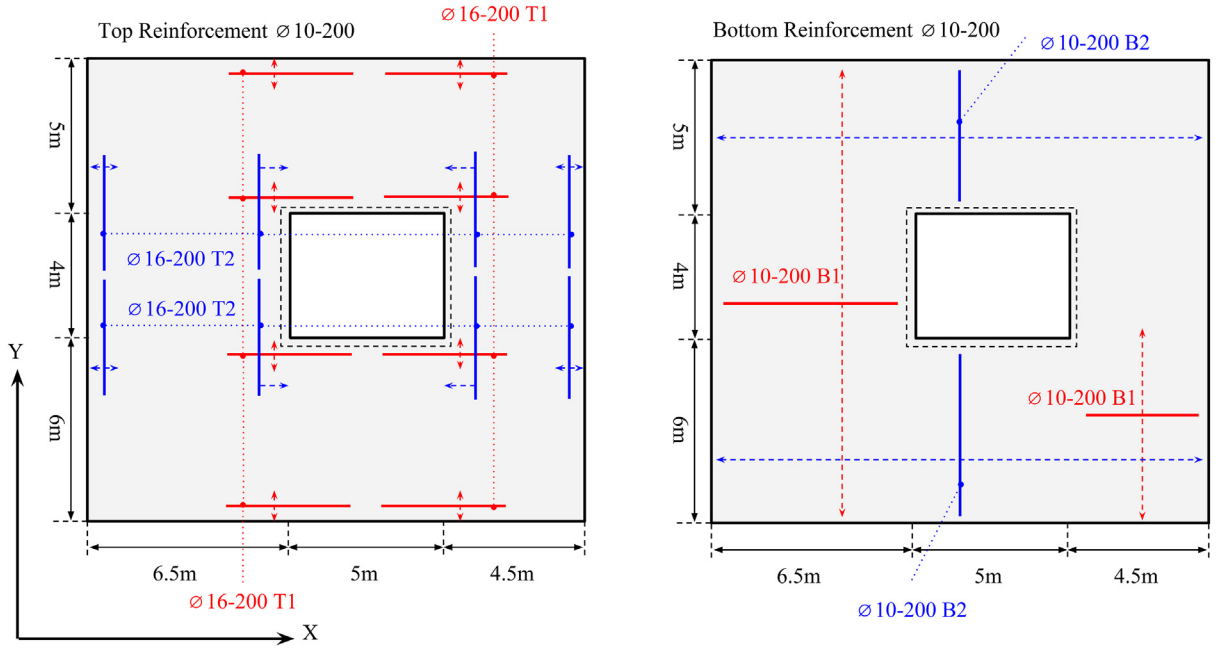

Fig. 11. Top and bottom reinforcement layouts for the conventional design. Blue and red lines are used to show the reinforcement bars on X- and Y-directions respectively. (For interpretation of the references to colour in this figure legend, the reader is referred to the web version of this article.)

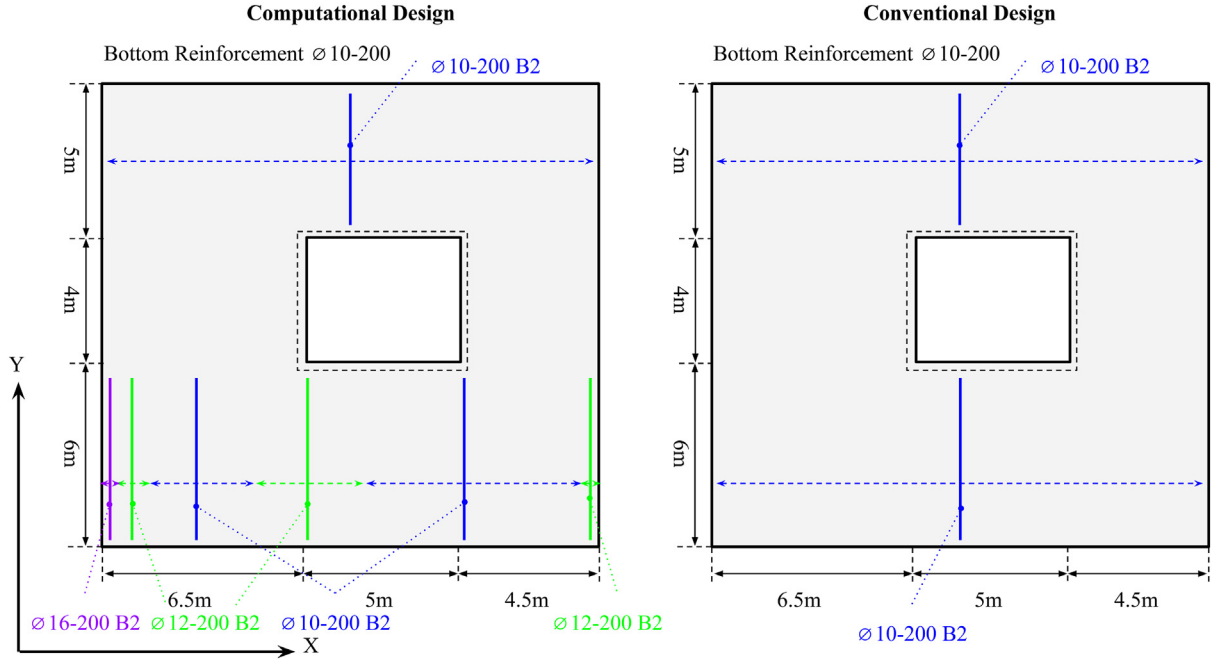

Fig. 12. Comparison of reinforcement layout (Bottom X) between the computational and the conventional approaches. The lines in blue colour correspond to ø10 at 200 mm reinforcement bars, in green colour to ø12 at 200 mm bars and in purple to ø16 at 200 mm bars. (For interpretation of the references to colour in this figure legend, the reader is referred to the web version of this article.)

4. Discussion and implementation

There is an increasing demand by engineering practitioners to optimise various elements of buildings structures, to improve efficiencies [24], reduce costs or enhance the environmental performance of their designs [32,33]. To effectively improve the current practices in common engineering projects most of the design specification procedures will have to be automated. The paper presented a computational approach that automates the reinforcement specification in RC floors supporting a BIM-based optimisation of RC structures.

4.1. Design and construction synergies

The proposed design optimisation and specification practices could create new synergies between design and construction processes like the one proposed by Bamtec Reinforcement [34] that allows engineers to more accurately design the reinforcement in concrete slabs with variable bars and spacing using rolling meshes. This technology can reduce the steel-fixing time of reinforcement, whilst offering steel savings by accommodating various combination of bars.

Additionally, in recent studies robotic technologies appear to improve the fabrication processes in the construction industry [35] and

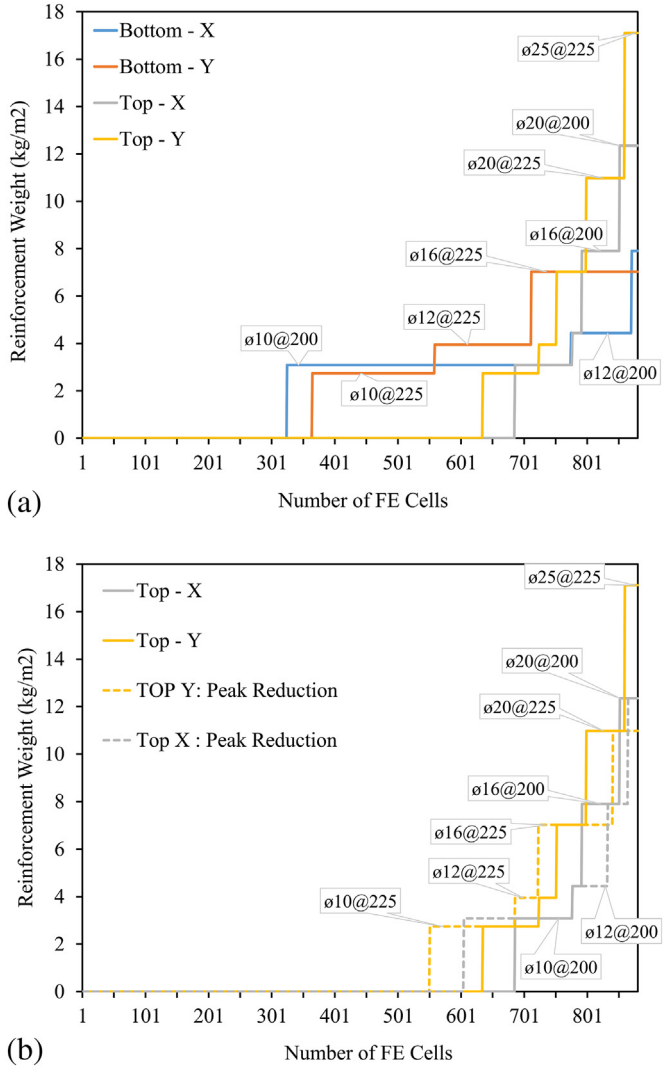

Fig. 13. (a) Summary of additional reinforcement options without peak reductions for top and bottom reinforcement in both directions, (b) Comparison between the obtained diameters for top reinforcement in both direction with (dotted lines) and without (solid lines) the peak reduction algorithm. In both figures, the horizontal axis shows in how many FE cells each reinforcement type occurs. The vertical axis shows the corresponding weight of the different reinforcement options in kg/m^2.

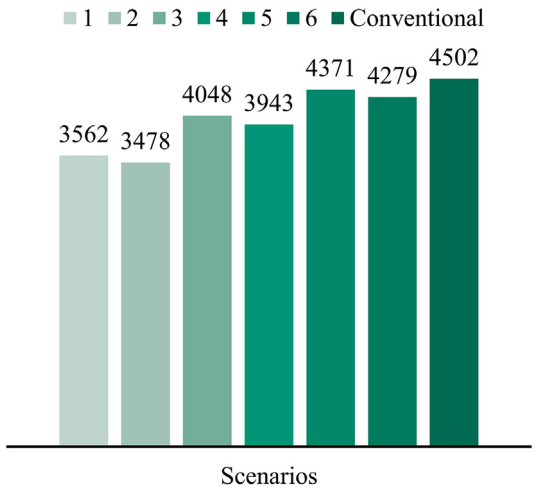

Fig. 14. Total reinforcement weight in kg for the six computed scenarios and the conventional scenario.

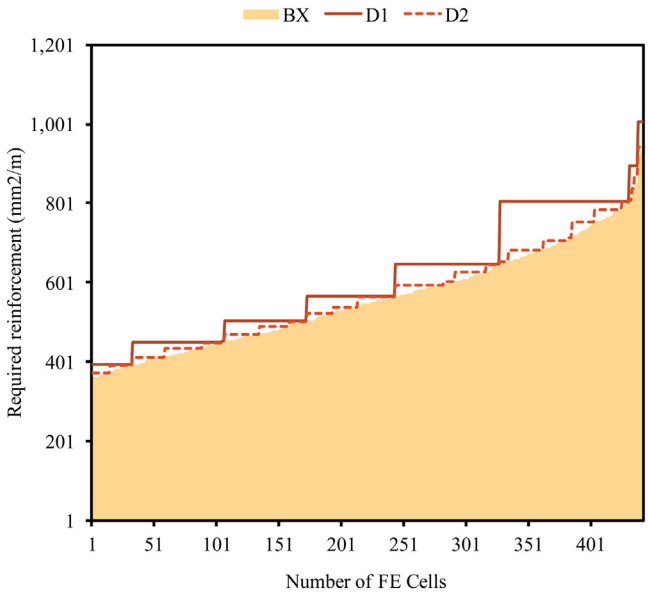

Fig. 15. Discrepancies between D1 (solid line) and D2 (dotted line) databases in the mapping of required reinforcement for the bottom reinforcement in X direction. Due to the larger number of spacing options in D2 database against D1, a closer approximation of the required reinforcement can be observed.

particularly in concrete structures [36], whilst allowing the construction of more complex reinforcement at little or no extra cost. Using the proposed reinforcement specification as an integrated front-end to these automated construction technologies has the potential to yield truly optimised engineering design workflows that can manage the increased complexity of building structures whilst enabling resource efficient and cost effective solutions in a timely manner.

4.2. Design collaboration

The traditional approaches for steel reinforcement specification require manual calculations, which are often time-consuming and error-prone. The rapid assessment of the required reinforcement in the slab could assist engineering practitioners in the early stages of the design development when various slab configurations are analysed in a short time. The time savings associated with the reinforcement analysis are expected to be considerable as manual data processing is not needed in the proposed approach. In addition to the increase in productivity, the parametric nature of the proposed specification significantly improves the collaboration with architects and contractors as frequent changes in the design could be accommodated in a cost-effective manner.

5. Conclusions

The study proposed an automated reinforcement specification approach that integrates code verification within a BIM-based optimisation procedure. The developed computational process used structural BIM data to initiate the FEM analysis, and it incorporated several smoothing functions applying constructability constraints to obtain designs of acceptable complexity. The practical dimensions of the new design model were evaluated in real building scenarios against solutions generated by structural engineering practitioners. It was found that the constructability constraints significantly influence the results. The proposed automated method can effectively achieve detailed reinforcement designs. In the future, the proposed automated design process could be integrated with new fabrication processes to achieve more efficient structural design systems overall.

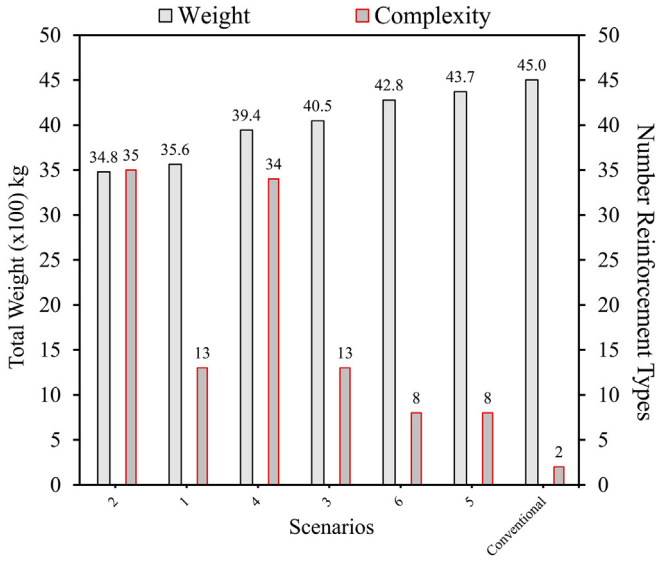

Fig. 16. Relationship between total reinforcement weight and design complexity.

Acknowledgements

This research has been made possible through funding provided by the Engineering and Physical Sciences Research Council (EPSRC) and from Price & Myers LLP via the UCL EngD Centre (Grant number: EP/G037159/1) in Virtual Environments, Interaction and Visualisation and this is gratefully acknowledged here.

References

[1] C. Coello, A. Christiansen, F. Santos Hernandez, A simple genetic algorithm for the design of reinforced concrete beams, Eng. Comput. 13 (4) (December 1997) 185–196, https://doi.org/10.1007/BF01200046.
[2] R. Rao, A material selection model using graph theory and matrix approach, Mater. Sci. Eng. A 431 (1–2) (September 2006) 248–255, https://doi.org/10.1016/j.msea.2006.06.006.
[3] A. Adedeji, Searching for the optimal design variables of RC flat slab by the reactive taboo, Trends Appl. Sci. Res. 6 (4) (2011) 375–385, https://doi.org/10.3923/tasr.2011.375.385.
[4] M. Mangal, J. Cheng, Automated optimization of steel reinforcement in RC building frames using building information modeling and hybrid genetic algorithm, Autom. Constr. 90 (June 2018) 39–57, https://doi.org/10.1016/j.autcon.2018.01.013.
[5] W. Bennage, A. Dhingra, Single and multiobjective structural optimization in discrete-continuous variables using simulated annealing, Int. J. Numer. Methods Eng. 38 (August) (1995) 2753–2773, https://doi.org/10.1002/nme.1620381606.
[6] M. Cohn, A. Divonitzer, Application of structural optimization, J. Struct. Eng. 120 (2) (1994) 617–650, https://doi.org/10.1061/(ASCE)0733-9445(1994)120:2(617).
[7] M. Jahjouh, M. Arafa, M. Alqedra, Artificial Bee Colony (ABC) algorithm in the design optimization of RC continuous beams, J. Struct. Multidiscip. Optim. 47 (6) (June 2013) 963–979, https://doi.org/10.1007/s00158-013-0884-y.
[8] W. Jenkins, Towards structural optimization via the genetic algorithm, Comput. Struct. 40 (5) (1991) 1321–1327, https://doi.org/10.1016/0045-7949(91)90402-8.
[9] G. Zavala, A. Nebro, F. Luna, C. Coello Coello, A survey of multi-objective metaheurtistics applied to structural optimization, Struct. Multidiscip. Optim. 49 (4) (April 2014) 537–558, https://doi.org/10.1007/s00158-013-0996-4.
[10] M. Bensdoe, O. Sigmund, Topology Optimisation: Theory, Methods and Applications, Springer, 2002, https://doi.org/10.1007/978-3-662-05086-6.
[11] F. Glover, Heuristic for integer programming using surrogate constraints, Decis. Sci. 8 (1) (January 1977) 156–166, https://doi.org/10.1111/j.1540-5915.1977.tb01074.x.
[12] M. Pincus, Monte Carlo method for the approximate solution of certain types of constrained optimization problems, Oper. Res. 18 (6) (November–December 1970) 967–1235, https://doi.org/10.1287/opre.18.6.1225.
[13] A. Tiwari, P. Hoyos, W. Hutabarat, C. Turner, N. Ince, X.-P. Gan, N. Prajapat, Survey on the use of computational optimisation in UK engineering companies, CIRP J. Manuf. Sci. Technol. 9 (January 2015) 57–68, https://doi.org/10.1016/j.cirpj.2015.01.003.
[14] B. Ahmadi-Nedushan, H. Varaee, Minimum cost design of concrete slabs using particle swarm optimization with time varying acceleration coefficients, World Appl. Sci. J. 13 (12) (2011) 2484–2494 (ISSN 1818-4952).
[15] M. Kripka, G. Medeiros, A. Lemonge, Use of optimization for automatic grouping of beam cross-section dimensions in reinforced concrete building structures, Eng. Struct. 99 (September 2015) 311–318, https://doi.org/10.1016/j.engstruct.2015.05.001.
[16] S. Eleftheriadis, D. Mumovic, P. Greening, Life cycle energy efficiency in building structures: a review of current developments and future outlooks based on BIM capabilities, Renew. Sust. Energ. Rev. 67 (January 2017) 811–825, https://doi.org/10.1016/j.rser.2016.09.028.
[17] S. Song, J. Yang, N. Kim, Development of a BIM-based structural framework optimization and simulation system for building construction, Comput. Ind. 63 (9) (December 2012) 895–912, https://doi.org/10.1016/j.compind.2012.08.013.
[18] J. Tulke, J. Hanff, 4D construction sequence planning – new process and data model, Proceedings of the CIB W078 24th International Conference on Information Technology in Construction, Maribor, Slovenia, 2007 [Online]. Available http://www.irbnet.de/daten/iconda/CIB21474.pdf , Accessed date: 1 October 2018.
[19] J. Tulke, M. Nour, K. Beucke, A dynamic framework for construction scheduling based on BIM using IFC, Proceedings of the 17th IABSE Congress, Chicago, USA, 2008, https://doi.org/10.2749/222137908796292119.
[20] H.-L. Chi, X. Wang, Y. Jiao, BIM-enabled structural design: impacts and future developments in structural modelling, analysis and optimisation processes, Arch. Comput. Meth. Eng. 22 (1) (January 2015) 135–151, https://doi.org/10.1007/s11831-014-9127-7.
[21] M. Aldwaik, H. Adeli, Cost optimization of reinforced concrete flat slabs of arbitrary configuration in irregular highrise building structures, Struct. Multidiscip. Optim. 54 (1) (July 2016) 151–164, https://doi.org/10.1007/s00158-016-1483-5.
[22] S. Eleftheriadis, P. Duffour, P. Greening, J. James, D. Mumovic, Multilevel computational model for cost and carbon optimisation of reinforced concrete floor systems, 34th International Symposium on Automation and Robotics in Construction (ISARC 2017), Taipei, Taiwan, 2017 9781510844735.
[23] M. Sahab, A. Ashour, V. Toropov, Cost optimisation of reinforced concrete flat slab buildings, Eng. Struct. 27 (3) (February 2005) 313–322, https://doi.org/10.1016/j.engstruct.2004.10.002.
[24] S. Eleftheriadis, P. Duffour, P. Greening, J. James, B. Stephenson, D. Mumovic, Investigating relationships between cost and CO_2 emissions in reinforced concrete structures using a BIM-based design optimisation approach, Energ. Buildings 166 (May 2018) 330–346, https://doi.org/10.1016/j.enbuild.2018.01.059.
[25] B. Saini, V. Sehgala, M. Gambhirb, Genetically optimized artificial neural network based optimum design of singly and doubly reinforced concrete beams, Asian J. Civil Eng. 7 (6) (2006) 603–619 [Online]. Available https://ajce.bhrc.ac.ir/Portals/25/PropertyAgent/2905/Files/6268/603.pdf , Accessed date: 1 October 2018.
[26] M. Hadi, Neural networks applications in concrete structures, Comput. Struct. 81 (6) (March 2003) 373–381, https://doi.org/10.1016/S0045-7949(02)00451-0.
[27] F. Ahmadkhanlou, H. Adeli, Optimum cost design of reinforced concrete slabs using neural dynamics model, Eng. Appl. Artif. Intell. 18 (1) (February 2005) 65–72, https://doi.org/10.1016/j.engappai.2004.08.025.
[28] A. Bond, O. Brooker, A. Fraser, A. Harris, T. Harrison, A. Jones, R. Moss, R. Narayanan, R. Webster, How to design concrete structures to eurocode 2 - the compendium, MPA The Concrete Centre, London, UK, (2011) [Online]. Available http://greganagno.com/download/Reinforced%20Concrete/How%20to%20design%20concrete%20structures%20using%20Eurocode%202.pdf , Accessed date: 1 October 2018.
[29] O. Brooker, How to design reinforced concrete flat slabs using Finite Element Analysis, MPA The Concrete Centre, London, UK, (2006) [Online]. Available https://www.concretecentre.com/Publications-Software/Publications/How-to-design-reinforced-concrete-flat-slabs-using.aspx , Accessed date: 1 October 2018.
[30] S. Coons, Surfaces for Computer-Aided Design of Space Forms, Massachusetts Institute of Technology, Cambridge, MA, USA, 1967 [Online]. Available http://www.dtic.mil/dtic/tr/fulltext/u2/663504.pdf , Accessed date: 1 October 2018.
[31] R. Wood, G. Armer, A. Hillerborg, The theory of the strip method for design of slabs, Proc. Inst. Civ. Eng. 41 (2) (1968) 285–311, https://doi.org/10.1680/iicep.1968.7755.
[32] S. Eleftheriadis, P. Duffour, D. Mumovic, BIM-embedded life cycle carbon assessment of RC buildings using optimised structural design alternatives, Energ. Buildings 173 (August 2018) 587–600, https://doi.org/10.1016/j.enbuild.2018.05.042.
[33] S. Eleftheriadis, Y. Schwartz, R. Raslan, P. Duffour, D. Mumovic, Integrated building life cycle carbon and cost analysis embedding multiple optimisation levels, Building Simulation and Optimization 2018, Cambridge, UK, 2018 [Online]. Available http://discovery.ucl.ac.uk/10056381/ , Accessed date: 1 October 2018.
[34] Bamtec, Bamtec system, [Online]. Available http://www.bamtec.com/Bamtec_en/Bamtec_System.htm, (2017) , Accessed date: 1 October 2018.
[35] T. Sandy, M. Giftthaler, K. Dorfler, M. Kohler, J. Bunchli, Autonomous repositioning and localization of an in situ fabricator, IEEE International Conference on Robotics and Automation (ICRA), Stockholm, Sweden, 2016, https://doi.org/10.1109/ICRA.2016.7487449.
[36] T. Wangler, E. Lloret, L. Reiter, N. Hack, F. Gramazio, M. Kohler, M. Bernhard, B. Dillenburger, J. Buchli, N. Roussel, R. Flatt, Digital concrete: opportunities and challenges, RILEM Tech. Lett. 1 (2016) 67–75, https://doi.org/10.21809/rilemtechlett.2016.16.